Review of Scientific Instruments ARTICLE pubs.aip.org/aip/rsi

Double-sided electron energy analyzer for measurement of non-Maxwellian electron energy distributions

Cite as: Rev. Sci. Instrum. 94, 123509 (2023); doi: 10.1063/5.0164402
Submitted: 22 June 2023 • Accepted: 16 November 2023 •
Published Online: 22 December 2023

Byungkeun Na,[1,a] Adam Robbins,[2] Jongsoo Yoo,[2] and Hantao Ji[2]

AFFILIATIONS

[1] Korea Institute of Fusion Energy, Daejeon 34133, Republic of Korea
[2] Princeton Plasma Physics Laboratory, Princeton, New Jersey 08543, USA

[a] Author to whom correspondence should be addressed: bna81@kfe.re.kr

ABSTRACT

A double-sided electron energy analyzer is developed for studies of magnetic reconnection. It can measure electron energy distribution functions along two directions opposite to each other at the same time. Each side is composed of a floating reference grid, an energy selector grid, and a collector plate. The voltage of the selector grid is swept from −40 to 0 V with respect to the reference grid with a frequency of 1 MHz. This fast sweeping is required to resolve sub-Alfvénic changes in plasma quantities of the Magnetic Reconnection Experiment, where the typical Alfvénic time is a few microseconds. The reliability of the energy analyzer is checked in Maxwellian plasmas away from the reconnection region. In this case, the electron temperature computed from the electron energy distribution function agrees with measurements of a reference triple Langmuir probe. When it is located near the reconnection region, the temperatures of the tail electron population from both sides, facing into the electron flow and facing away from it, exceed the bulk electron temperature measured by the Langmuir probe by a factor of about 2.

I. INTRODUCTION

Magnetic reconnection is a fundamental process in magnetized plasmas, during which magnetic field lines are rearranged and the magnetic energy is converted to particle energy.[1] Magnetic reconnection has been widely believed to be responsible for energetic electron generation in space and laboratory plasmas. For example, the RHESSI spacecraft observed that a significant fraction (up to 50%) of the magnetic energy is converted to energetic electrons,[2] and *in situ* measurements in the magnetosphere show a positive correlation between reconnection and energetic particle generation.[3] Energetic electrons associated with magnetic reconnection have been also observed in laboratory plasmas; Stenzel *et al.* reported runaway-type fast electrons inside a current sheet with a large guide field.[4] Non-thermal electrons have been also observed during sawtooth crashes and disruptions in hot tokamak plasmas.[5]

Energetic electron generation during reconnection has not been thoroughly studied in the Magnetic Reconnection Experiment (MRX)[6] because of the lack of proper diagnostics. Possible diagnostics include an electron energy analyzer (EEA), which has been used for studies of reconnection in other devices.[4,7] In MRX, the development of an EEA system is challenging due to two technical difficulties. First, there is no well-defined reference (ground) for the system since the plasma potential swings from −150 to 100 V during the discharge. Second, measurements of the electron energy distribution function (EEDF) have to be conducted very fast (within 1 μs) because the relevant plasma quantities, such as the electron temperature (T_e) and density (n_e), are locally changing on the order of a microsecond.

For studies of energetic electron generation in MRX, a double-sided electron energy analyzer (DSEEA) has been developed.[8] To overcome the aforementioned technical difficulties, the DSEEA has a floating grid which provides a reference voltage for the rest of the system. The selector bias voltage is swept with a 1 MHz frequency with respect to the reference voltage by using amplifiers and transformers. To check its validity, EEA measurements are compared to those of a nearby triple Langmuir probe (LP) in Maxwellian plasmas. Then, the DSEEA is used to measure the temperature of the electron

tail population near the reconnection region. In Sec. II, the setup of MRX and the DSEEA system is described. Results from the DSEEA are presented in Sec. III. Finally, future use of the DSEEA for studies of reconnection is discussed in Sec. IV.

II. EXPERIMENTAL SETUP

A. Magnetic Reconnection Experiment

MRX is a mid-size laboratory device specifically designed for detailed studies of magnetic reconnection. Figure 1(a) shows a cutaway view of the MRX vacuum chamber. The local coordinate system is also shown: R is radially outward, Y is the out-of-plane direction, and Z is the axial direction. The gray circles in Fig. 1(a) indicate cross sections of donut-shaped flux cores inside which there are two sets of coils: poloidal field (PF) coils and toroidal field (TF) coils. The PF coils are wound toroidally to generate the X-line geometry at the middle of the MRX device and to drive magnetic reconnection.[6] The TF coils are wound poloidally to inductively create the plasma around the flux cores. The red circles in Fig. 1(a) are drive (DR) coils, which provide additional magnetic reconnection drive.[9] Typical plasma parameters are as follows: electron density, $n_e = 10^{13}$–10^{14} cm^{-3}; electron temperature, $T_e = 5$–15 eV; magnetic field strength, $B = 0.2$–1 kG; Lundquist number, $S = 200$–500. For this study, helium is used with about 4.5 mTorr of fill pressure.

Various *in situ* diagnostics are used in MRX, including a magnetic probe array, triple Langmuir probes (LP), and Mach probes.[10] The magnetic probe array, which is the main diagnostic of MRX, measures 2-D profiles of all three components of the magnetic field, which can be used to obtain the current density ($\vec{J} = \nabla \times \vec{B}/\mu_0$). Triple Langmuir probes (LP)[11] measure the electron density and temperature, and Mach probes provide the local ion flow velocity. A DSEEA is inserted in the plasma together with a Langmuir probe, which has the same R and Z position as the DSEEA but is separated along the symmetric (Y) direction by 4 cm. This reference Langmuir probe provides important information regarding the bulk electron temperature.[12]

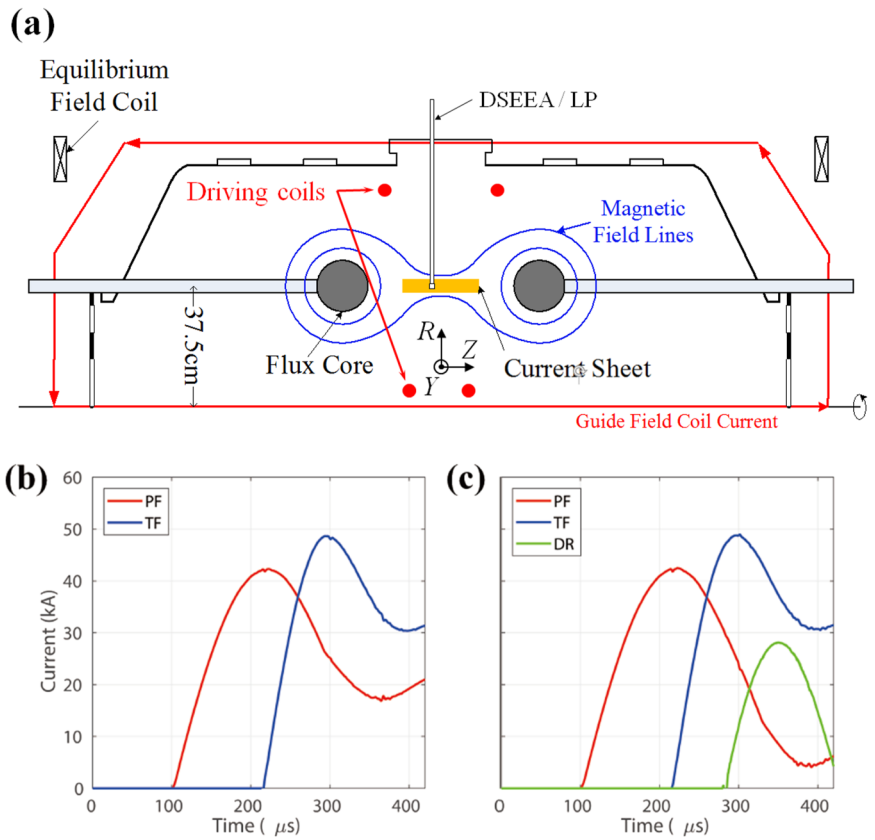

FIG. 1. (a) Schematic view of the Magnetic Reconnection Experiment (MRX). Poloidal field (PF) and toroidal field (TF) coils exist inside flux cores (gray circles) to drive magnetic reconnection and to generate a plasma, respectively. Drive coils (DR) are also installed for further reconnection drive. The current sheet is elongated along the Z direction. Sample magnetic field lines in MRX are also illustrated by blue curves. (b) Current waveforms of the PF and TF coils for Maxwellian plasmas. To reduce effects from magnetic reconnection, the data are acquired at the upstream around 304 μs when magnetic reconnection is not yet driven. (c) Current waveforms of the PF, TF, and DR coils for energetic electron generation. Magnetic reconnection is strongly driven by the time-varying PF and DR coil currents.

B. DSEEA

Figure 2(a) shows a schematic diagram of the DSEEA. Two independent and separated EEAs are combined for simultaneous measurements of the electron energy distributions along two directions opposite to each other. Each side is composed of two grids and a collector, separated by mica plates. Note that there are only two grids rather than four grids, which are typical for conventional retarded potential energy analyzers.[13,14] In most pulsed plasmas as in MRX, energy analyzers use fewer than four grids to secure a sufficient amount of current.[7,15] The probe head is electrically floating to minimize the perturbation by the probe. The first (reference) grid is also floating, and voltages of the second (selector) grid and the collector plate are biased with respect to the voltage of the first grid. Since the reference grid is floating, the bulk population of electrons with energy less than the difference between the plasma (V_p) and floating potential (V_f) is rejected at the reference grid. The relation between V_p and V_f is given by $V_p - V_f = (3.3 + 0.5 \ln \mu) T_e$.[16] Here, $\mu = m_i/m_p$ is the ratio between the ion and proton mass, and T_e is in units of eV. Because of this rejection of bulk electrons at the reference grid, the DSEEA cannot provide data for the bulk electron temperature, which is separately measured by the nearby LP. The voltage of the selector grid (V_{sel}) with respect to the floating grid is swept from −40 to 0 V with a frequency of 1 MHz. The selector grid rejects electrons with energy less than its voltage. Furthermore, the collector grid is biased at a high voltage of +54 V with respect to the floating grid to collect electrons that pass through the selector grid and to reject most ions. Due to the potential profile inside the probe as shown in Fig. 2(a), the secondary electrons emitted from the collector are reflected by the electric field between the selector and the collector. The collector bias voltage (V_{col}) was experimentally determined: the collector current was saturated at $V_{col} > 50$ V with $V_{sel} = 0$. When V_{col} is too high (>80 V), arcing between the floating grid and the collector plate occurred, which damaged the DSEEA. Finally, the collector plates are oriented along the magnetic field line. This is necessary to avoid the large polarization currents generated by the fast-sweeping selector potential.[17]

The grids are covered by a 7 mm square stainless steel plate with a 2.8 mm diameter circular hole at the center. Its role is to mechanically protect the grids and to limit the electron current. The hole size is determined to obtain a reasonable signal-to-noise ratio. The maximum collector current is expected to be about 70 mA in a typical MRX plasma with $T_e = 10$ eV and $n_e = 3 \times 10^{13}$ cm^{-3}. The size of the stainless steel plate is determined such that it stays at the floating potential regardless of the current to the grids. Since the surface to the hole area ratio is about 8:1, and the grid transparency is about 50%, the first grid becomes close to the floating potential within 1% regardless of the collector current.

The grids are made of a fine-wire nickel mesh. Mica plates are used to insulate among the grids and collector, and their thickness is about 0.8 mm. The collector is made of a copper plate. The whole structure is glued together with a vacuum-compatible epoxy. The complete assembly is shown in Fig. 2(a). For the design of the EEA, the wire line width (distance between two adjacent wires) of the mesh and material are important. The line width should satisfy the criterion, $d < 2 \times \lambda_D$,[13] where d is the line width and λ_D is the Debye length. In this study, the mesh with $d = 18$ μm is used due to its commercial availability, even though the line width should be less than 14 μm for a typical MRX plasma to satisfy the criteria. In this case, the equipotential surface at each grid can be bumpy, such that the electron propagation can be deflected. A nickel mesh is used due to its commercial availability for the requisite spacing. While nickel is magnetic, the effects are negligible: the mesh is too small to influence the larger MRX fields, and the energy selection process is undisturbed by the local field perturbation (though the effective transparency may be reduced).

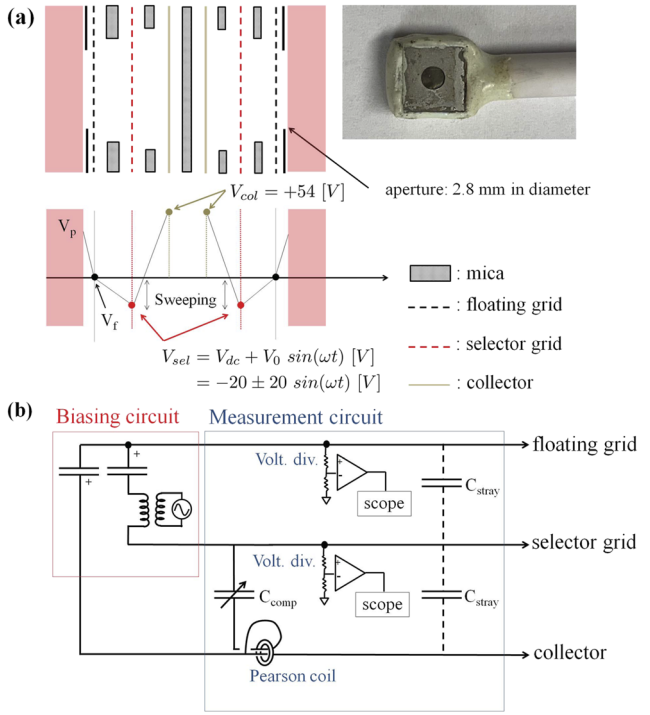

FIG. 2. (a) Schematic of the probe head of the DSEEA. Each side is composed of two grids and a collector separated by mica plates. A photograph of the DSEEA with a shaft after use is at the right top. (b) Circuit diagram of each side of the DSEEA. The circuit supplies DC and AC biases to grids and collectors with respect to the floating (reference) grid. The selector voltage and collector currents are measured. Effects from the stray capacitance between the selector and collector on the current measurement are compensated by an adjustable compensation capacitor.

Figure 2(b) shows a circuit diagram for the EEA. The reference grid is at the floating potential of the plasma and the collector is biased at $V_{col} = +54$ V by a 3.3 mF capacitor to reject the ions. The selector grid bias is also controlled by a 3.3 mF capacitor, which provides a −20 V bias. An amplified sine wave signal is added through a 1:1 transformer, which is required to separate the circuit from the ground. Adding these together, the selector voltage is given by $V_{sel} = -20 + 20 \sin(2\pi f t)$ V, where the sweeping frequency f is 1 MHz. The voltage difference between the floating grid and the selector grid is measured by an oscilloscope via voltage dividers. The collector current is also measured by an oscilloscope via a Pearson current monitor. As a result, an I–V curve is acquired during a half period of the voltage sweeping, 0.5 μs.

The collector current should be compensated since it includes an unwanted current from stray capacitance between the selector and the collector cables. A variable compensation capacitor is connected between the selector and the collector, and the cable passes through the Pearson coil in the opposite direction of the stray current, such that the compensation current cancels the stray current.[18] The compensation capacitance is experimentally determined by minimizing the collector currents without plasmas. The circuit is connected to the probe head a few seconds before the plasma is created, and the circuit is disconnected from the probe head and connected to the DC power supply, such that the capacitors are recharged between discharges.

There are two methods to obtain the electron energy distribution from the I–V curve, the collector current vs. the selector bias voltage. One method is the exponential fitting of the I–V curve, which works only for the Maxwell distribution. The other is the differentiation of the I–V curve, which works even for non-Maxwellian distributions. Since the goal of this study is to measure non-Maxwellian electrons, the differentiation method is chosen. In general, the electron current to the collector is described as follows:

$$I_{\rm col} = -A_{\rm eff} e \int_{v_{\rm min}}^{\infty} v f(v) dv \tag{1}$$

$$= -A_{\rm eff} \frac{e}{m_e} \int_{E_{\rm sel}}^{\infty} f(E)\, dE, \tag{2}$$

where $A_{\rm eff}$ is the effective area of the EEA collector, m_e is the electron mass, $E_{\rm sel} = eV_{\rm sel}$ is the relative electron energy corresponding to the selector bias, and $f(E)$ is an arbitrary electron energy distribution. Note that $f(E) = f(v = \sqrt{2E/m})$ is mathematically still a velocity distribution, i.e., it quantifies the electron density per unit speed, not per unit energy. Then, the electron energy distribution is acquired by differentiating both sides,

$$f(E) = \frac{1}{A_{\rm eff}} \frac{m_e}{e^2} \frac{dI_{\rm col}}{dV_{\rm sel}}. \tag{3}$$

III. RESULTS

A. Functionality of the DSEEA in Maxwellian plasmas

To check its validity, the DSEEA has been tested in Maxwellian plasmas. To make sure the local electron distribution is Maxwellian, the DSEEA is located at $R = 43.5$ cm, which is about $2d_i$ away from the current sheet $R \sim 37.5$ cm. Here, d_i is the ion skin depth. To further decrease effects from magnetic reconnection, the reconnection drive has been suppressed by controlling the PF waveform. The reconnection drive is determined by the slope of the PF current. As shown in Fig. 1(b), the change in the PF current is minimized at 300 μs, around which data from the DSEEA are analyzed and compared to data from a nearby LP. Under this condition, the local electric field is minimal, such that the local electron distribution function is Maxwellian. The local electron-ion collision frequency is about 1 MHz.

Figures 3(a) and 3(b) show examples of the selector bias voltages and the collector currents from EEA1 and EEA2, referring to each side of the DSEEA. The selector bias voltage is swept from 0 to −35 V with 1 MHz, and the collector current varies according to the selector bias voltage. Due to the stray capacitance, noisy current signals are seen, for example, near 304 μs. Even though this effect is minimized by controlling the compensation capacitor as described in Sec. II B, the signal-to-noise ratio is quite low when the collector current is minimal. When the selector bias voltage is higher than −20 V, this effect is ignorable.

The resultant I–V curves from EEA1 and EEA2 are shown in Figs. 3(c) and 3(d). As expected in Maxwellian plasmas, the collector current exponentially decreases with respect to the electron energy. In each curve, 12 I–V curves are chosen from similar plasma conditions in terms of plasma parameters and are statistically processed to find a proper error range. The horizontal axis is the electron energy $E_e = V_p - V_f - V_{\rm sel}$. Here, $V_p - V_f = 4T_e$ is acquired from the LP measurement. Since the electron temperature is about 12 eV, the population of electrons with energy lower than 48 eV cannot be measured.

Figures 3(e) and 3(f) show the electron energy distribution calculated from Figs. 3(c) and 3(d), respectively. The electron temperatures from EEAs are acquired by exponential fitting of the electron energy distributions, but the high energy (>66 eV) part is excluded due to the low signal-to-noise ratio in the I–V curve. The average bulk electron temperature measured by the LP is $T_e = 11.9$ eV, while the temperatures of the electron tail populations by EEA1 and EEA2 are 13.1 and 13.0 eV, respectively. Thus, the temperature measured by the DSEEA agrees with LP measurements within errors. Typically, the error of LP measurement is about 10%, while that of the DSEEA is 10%–20% due to errors from the signal processing, noise filtering, and smoothing, which is necessary to reduce spikes after differentiation of the I–V curve.

B. Electron energy distributions in the current sheet

The main goal of the DSEEA is to measure the temperature of energetic electrons in the current sheet where magnetic reconnection occurs. Various locations and directions should be investigated to find the energetic electrons because the possible acceleration mechanisms exist at different locations. One possibility is direct acceleration by the strong out-of-plane reconnection electric field. To create such a situation, reconnection is driven strongly by PF and DR currents. As shown in Fig. 1(c), the slope of the PF current around 326 μs is larger than the previous case. Moreover, the DR coils are used to provide further drive of reconnection.[9] The measurement is performed when the out-of-plane reconnection electric field is the strongest ($E_Y \sim 115$ V/m). The DSEEA is located at $R = 37.5$ cm near the reconnection region, facing the Y (out-of-plane) direction to acquire electron energy distributions along the reconnection electric field direction. EEA2 and EEA1 are facing into and away from the electron flow, respectively.

The electron energy distributions measured by the EEA1 and EEA2 are shown in Fig. 4. Unlike the previous case, EEDFs from EEA1 and EEA2 are different from each other. First, the population of the electron tail is significantly larger when EEA is facing into the electron flow (EEA2). Since the energy corresponding to the electron flow velocity ($\sim 10^5$ m/s) is much less than 0.1 eV, the difference is not mainly caused by the electron flow. The perturbation by the floating potential difference between the two sides is minimized as well since the difference is less than 0.1 eV. The blocking effect by the probe head is also unlikely to cause this large difference. Since ions are moving the other direction in the current sheet and ions

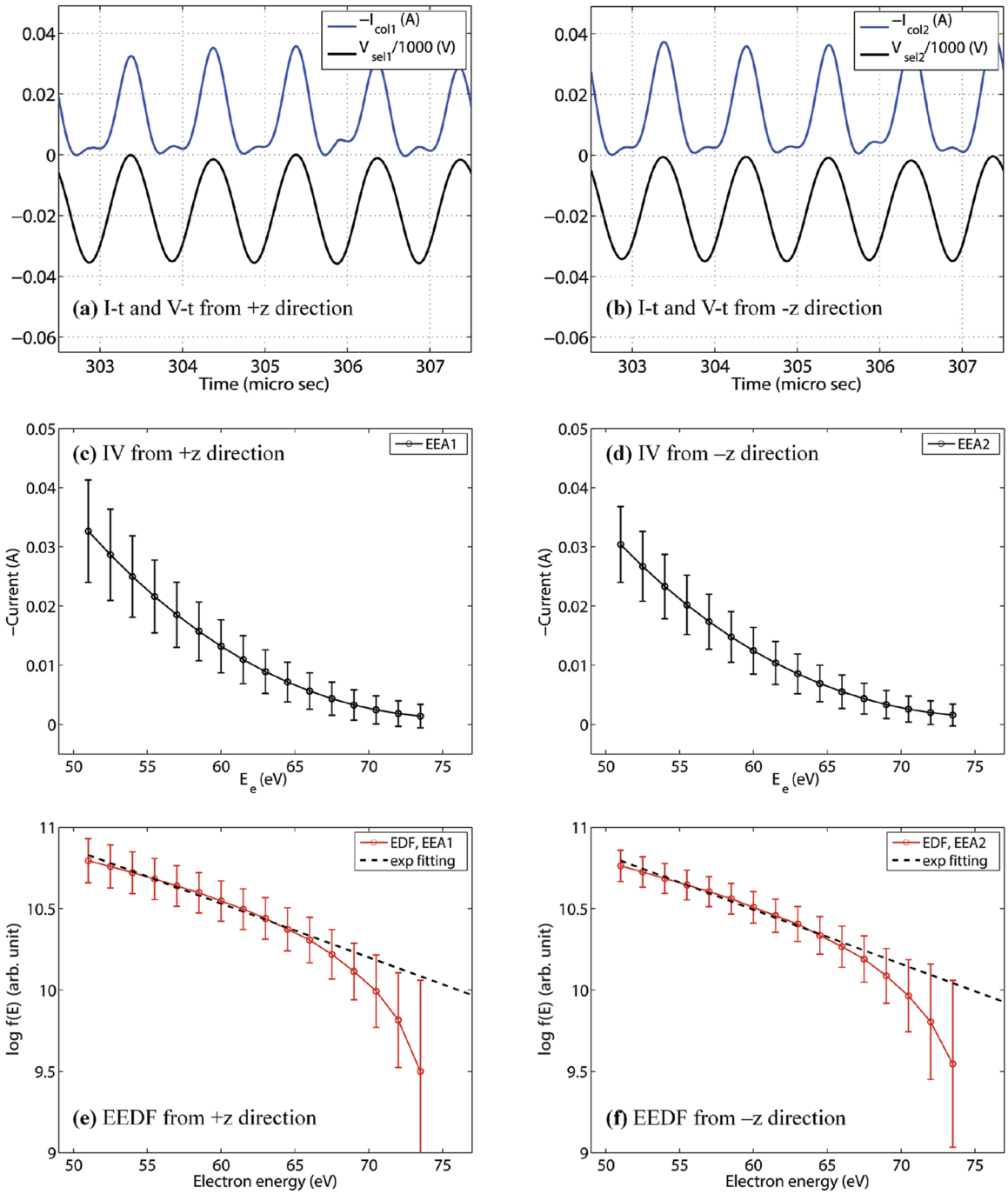

FIG. 3. (a) and (b) Examples of the selector bias voltage and the collector current with respect to time. They are measured from discharge #166917, and the data at 304.4–305.4 μs are used for the statistics in (c)–(f). Small noise signals arise when V_{sel} is minimal, and they stem from the stray capacitance and the compensation capacitor described in Sec. II B. This effect is minimized by controlling the compensation capacitor when the plasma is off. (c)–(f) I–V curves and electron energy distribution functions in a Maxwellian plasma. They are measured by EEA1 for (c) and (e) and by EEA2 for (d) and (f). The dashed line in (e) and (f) stands for a fit to a Maxwellian distribution function. There is no noticeable difference between measurements by EEA1 and EEA2. The measured tail temperatures are 13.1 and 13.0 eV, respectively, which is similar to the electron temperature by the reference Langmuir probe.

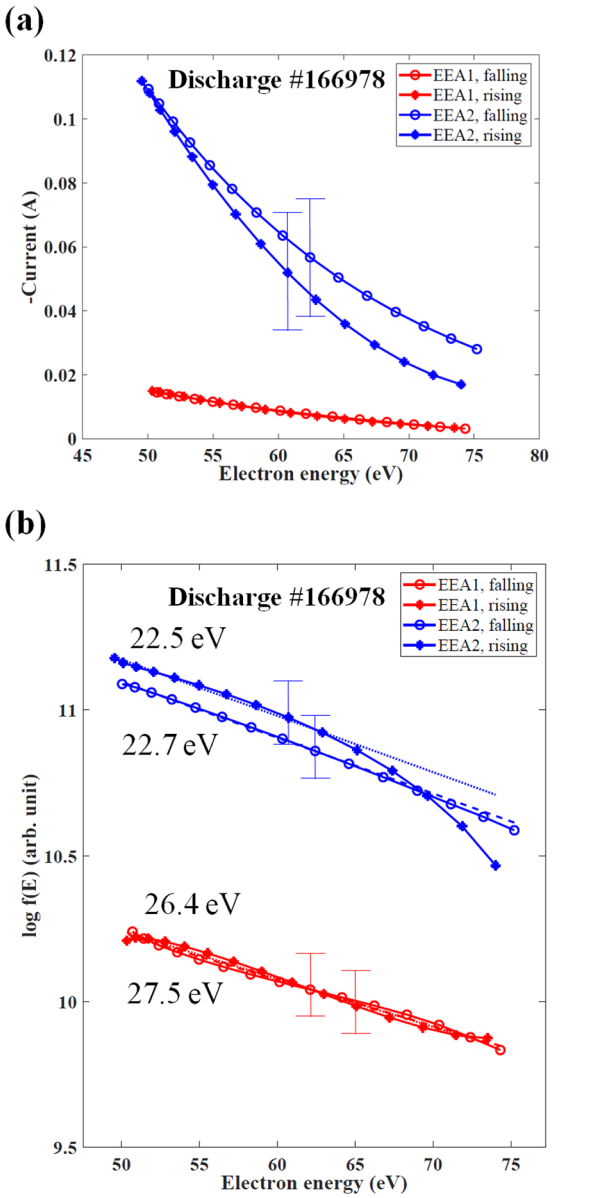

FIG. 4. (a) IV curves from EEA1 and EEA2. (b) Electron energy distribution functions measured in a current sheet during strongly-driven reconnection. The red and blue curves indicate EEDFs from EEA1 and EEA2, respectively. Dashed lines are fits to a Maxwellian distribution function. Curves with circles are EEDFs when the selection voltage rises, while those with asterisks are EEDFs when the bias voltage falls. In both figures, the horizontal axis for electron energy is conveniently scaled by assuming a floating potential of four times the electron temperature from the Langmuir probe. However, in reality, the horizontal axis is shifted with an unknown offset. The unknown offsets of EEA1 and EEA2 could be different from each other since they are electrically isolated. The tail electron temperature is significantly higher than the Langmuir probe measurement, 12.4 eV, while the tail temperature when EEA faces into the electron flow is slightly lower than when EEA faces away from the electron flow.

mostly control the density, the sheath density of EEA1 facing into the ion flow is expected to be higher than that of EEA2. Thus, the development of the tail population is indeed stronger along the electron flow direction, which indicates that the electron tail population is generated by the direct acceleration of electrons by the out-of-plane reconnection electric field.

The temperature of the electron tail population is also higher along the electron flow direction. The temperature measured by EEA2 is 22.7 eV when the selection bias voltage rises, while it is 22.5 eV when it falls. On the other hand, the tail temperature measured by EEA1 is 27.5 and 26.4 eV, respectively. The bulk electron temperature measured by the reference Langmuir probe is 12.4 eV. In both cases, the tail temperature is higher than the bulk electron temperature, which shows clear development of a hot tail population during reconnection. This high electron temperature persists for about 10 μs, during which the reconnection electric field stays high (~115 V/m) and the bulk electron temperature from the Langmuir probe remains around 12 eV.

Since energetic electrons are found, it is important to address the offset of the horizontal axis in Fig. 4. In Fig. 4, the horizontal axis is conveniently set based on the assumption that the floating potential is four times the electron temperature from the Langmuir probe. This scaling approach is employed despite the existence of energetic electrons. A more precise estimation of the offset requires the determination of the difference between the plasma potential and the floating potential. In principle, this can be done via direct measurement or inference from other plasma parameters (species densities, drift speeds, etc.), but suitable methods are not currently available in MRX. Since the Maxwellian tail temperature depends only on the slope of the distribution plots, our argument regarding the electron tail temperatures remains valid.

IV. DISCUSSION

A DSEEA is developed to measure the electron energy distribution from the two opposite directions for studies of energetic electron generation during magnetic reconnection. Due to special conditions of the MRX plasma, it is designed to have the selector bias swept from −40 to 0 V with respect to the reference floating potential with 1 MHz frequency. This fast sweeping is required to resolve the sub-Alfvénic change in plasma parameters, such as the density and temperature. The reference of the system also has to be the floating potential since the plasma potential of MRX plasma changes quickly from −150 to 100 V. In this case, serious arcing inside the EEA will damage it if the ground provides the reference voltage.

To check its validity, the DSEEA is inserted into a Maxwellian plasma. In this case, data from the DSEEA agrees with that from a reference LP within error bars. It should be mentioned that errors in DSEEA measurements are high (~20%) from signal processing. When the DSEEA is placed in an active current sheet, the measured tail temperature is much higher than the bulk electron temperature from the LP. The development of the energetic tail is much more significant when the EEA faces into the electron flow direction.

Although the sweeping frequency is high at 1 MHz, it is sometimes not sufficient when key plasma parameters change on

a microsecond time scale. This rapid change in plasma parameters occasionally occurs when the DSEEA is placed near the electron diffusion region where electron-scale structures may exist. This fast change in plasma parameters may explain the EEDF shape measured by EEA2. As shown in Fig. 4(b), the high energy part of EEA2 when the selector bias voltage is rising, which is measured at the end of the sweeping cycle, cooled rapidly. Another possibility is effects from the parasitic inductance and capacitance in the circuit. At frequencies higher than 1 MHz, these effects become noticeable. Future work is needed to minimize the stray inductance/capacitance in the circuit to achieve higher sweeping frequencies.

ACKNOWLEDGMENTS

This work was supported by the US DOE (Contract No. DE-AC0209CH11466) and the KSTAR Experimental Collaboration and Fusion Plasma Research (Grant No. EN2301-14) through the Korea Institute of Fusion Energy (KFE) funded by the Korean Government. The authors thank R. Cutler for technical support.

AUTHOR DECLARATIONS

Conflict of Interest

The authors have no conflicts to disclose.

Author Contributions

Byungkeun Na: Data curation (lead); Formal analysis (lead); Writing – original draft (lead). **Adam Robbins**: Visualization (supporting); Writing – review & editing (supporting). **Jongsoo Yoo**: Data curation (supporting); Formal analysis (supporting). **Hantao Ji**: Supervision (lead).

DATA AVAILABILITY

The data that support the findings of this study are openly available in the Princeton Data Commons at https://doi.org/10.34770/8ad7-jj80.[19]

REFERENCES

[1] E. R. Priest and T. Forbes, *Magnetic Reconnection: MHD Theory and Applications* (Cambridge University Press, New York, 2000).
[2] R. P. Lin, S. Krucker, G. J. Hurford, D. M. Smith, H. S. Hudson, G. D. Holman, R. A. Schwartz, B. R. Dennis, G. H. Share, R. J. Murphy, A. G. Emslie, C. Johns-Krull, and N. Vilmer, Astrophys. J. **595**, L69 (2003).
[3] M. Øieroset, R. P. Lin, T. D. Phan, D. E. Larson, and S. D. Bale, Phys. Rev. Lett. **89**, 195001 (2002).
[4] R. L. Stenzel, R. Williams, R. Agüero, K. Kitazaki, A. Ling, T. McDonald, and J. Spitzer, Rev. Sci. Instrum. **53**, 1027 (1982).
[5] P. V. Savrukhin, Plasma Phys. Controlled Fusion **48**, B201 (2006).
[6] M. Yamada, H. Ji, S. Hsu, T. Carter, R. Kulsrud, Y. Ono, and F. Perkins, Phys. Rev. Lett. **78**, 3117 (1997).
[7] W. Fox, M. Porkolab, J. Egedal, N. Katz, and A. Le, Phys. Plasmas **17**, 072303 (2010).
[8] A similar method has been developed in the MST reversed-field pinch plasma. See: M. R. Stoneking, S. A. Hokin, S. C. Prager, G. Fiksel, H. Ji, and D. J. Den Hartog, Phys. Rev. Lett. **73**, 549 (1994).
[9] J. Jara-Almonte, H. Ji, M. Yamada, J. Yoo, and W. Fox, Phys. Rev. Lett. **117**, 095001 (2016).
[10] J. Yoo, M. Yamada, H. Ji, and C. E. Myers, Phys. Rev. Lett. **110**, 215007 (2013).
[11] S.-L. Chen and T. Sekiguchi, J. Appl. Phys. **36**, 2363–2375 (1965).
[12] The bulk electron temperature may be different from the triple LP measurement since the measurement is affected by the non-Maxwellian tail as well. However, the non-Maxwellian electron population seems ignorable compared to the bulk electron population under this experimental condition since any significant change is not seen when the non-Maxwellian electron started to be generated. Therefore, we used the term, "the bulk electron," for convenience.
[13] C. Böhm and J. Perrin, Rev. Sci. Instrum. **64**, 31 (1993).
[14] G. D. Conway, A. J. Perry, and R. W. Boswell, Plasma Sources Sci. Technol. **7**, 337 (1998).
[15] R. A. Pitts, R. Chavan, S. J. Davies, S. K. Erents, G. Kaveney, G. F. Matthews, G. Neill, J. E. Vince, and I. Duran, "Retarding field energy analyzer for the JET plasma boundary," Rev. Sci. Instrum. **74**, 4644 (2003).
[16] I. H. Hutchinson, *Principles of Plasma Diagnostics*, 2nd ed. (Cambridge University Press, Cambridge, 2005).
[17] R. B. Lobbia and A. D. Gallimore, Phys. Plasmas **17**, 073502 (2010).
[18] This method has been used in previous studies. See e.g., P. R. Smy, J. A. Nation, and D. Simpson, J. Phys. D: Appl. Phys. **2**, 1095 (1969); B. M. Oliver, R. M. Clements, and P. R. Smy, J. Appl. Phys. **41**, 2117 (1970); F. W. Crawford, *ibid.* **34**, 1897 (1963).
[19] The data used in this study are found in the Princeton Data Commons. See https://doi.org/10.34770/8ad7-jj80 for the data of Figs.3 and 4.